Geophysical Research Letters

RESEARCH LETTER
10.1029/2024GL110691

Key Points:

- GPS data reveal summer speed up at least 190 km inland along the main flowline of Zachariae Isstrøm
- Subglacial hydrology is the main driver of the summer speedup near the terminus and deep inland
- Record high warming in 2019 led to a more intense and longer duration of the summer speedup

Supporting Information:

Supporting Information may be found in the online version of this article.

Correspondence to:

S. A. Khan,
abbas@space.dtu.dk

Citation:

Khan, S. A., Morlighem, M., Ehrenfeucht, S., Seroussi, H., Choi, Y., Rignot, E., et al. (2024). Inland summer speedup at Zachariæ Isstrøm, northeast Greenland, driven by subglacial hydrology. *Geophysical Research Letters*, *51*, e2024GL110691. https://doi.org/10.1029/2024GL110691

Received 13 JUN 2024
Accepted 7 SEP 2024

Author Contributions:

Data curation: Shfaqat A. Khan
Formal analysis: Shfaqat A. Khan, Mathieu Morlighem, Shivani Ehrenfeucht, Helene Seroussi, Youngmin Choi
Funding acquisition: Shfaqat A. Khan
Investigation: Shfaqat A. Khan
Methodology: Shfaqat A. Khan, Shivani Ehrenfeucht, Eric Rignot, Angelika Humbert
Project administration: Shfaqat A. Khan
Resources: Shfaqat A. Khan, Eric Rignot, Angelika Humbert
Software: Mathieu Morlighem, Shivani Ehrenfeucht, Helene Seroussi, Youngmin Choi
Supervision: Mathieu Morlighem

© 2024. The Author(s).
This is an open access article under the terms of the Creative Commons Attribution-NonCommercial-NoDerivs License, which permits use and distribution in any medium, provided the original work is properly cited, the use is non-commercial and no modifications or adaptations are made.

Inland Summer Speedup at Zachariæ Isstrøm, Northeast Greenland, Driven by Subglacial Hydrology

Shfaqat A. Khan[1], Mathieu Morlighem[2], Shivani Ehrenfeucht[3,4], Helene Seroussi[5], Youngmin Choi[6], Eric Rignot[3,7], Angelika Humbert[8,9], Derek Pickell[2], and Javed Hassan[1]

[1]DTU Space, Technical University of Denmark, Lyngby, Denmark, [2]Department of Earth Sciences, Dartmouth College, Hanover, NH, USA, [3]Department of Earth System Science, University of California-Irvine, Irvine, CA, USA, [4]Department of Geography and Environmental Management, University of Waterloo, Waterloo, ON, Canada, [5]Thayer School of Engineering, Dartmouth College, Hanover, NH, USA, [6]Earth System Science Interdisciplinary Center, University of Maryland, College Park, MD, USA, [7]Jet Propulsion Laboratory, California Institute of Technology, Pasadena, CA, USA, [8]Glaciology Section, Alfred Wegener Institute Helmholtz Centre for Polar and Marine Research, Bremerhaven, Germany, [9]Department of Geosciences, University of Bremen, Bremen, Germany

Abstract The Northeast Greenland Ice Stream (NEGIS) has experienced substantial dynamic thinning in recent years. Here, we examine the evolving behavior of NEGIS, with focus on summer speedup at Zachariae Isstrøm, one of the NEGIS outlet glaciers, which has exhibited rapid retreat and acceleration, indicative of its vulnerability to changing climate conditions. Through a combination of Sentinel-1 data, in-situ GPS observations, and numerical ice flow modeling from 2007, we investigate the mechanisms driving short-term changes. Our analysis reveals a summer speedup in ice flow both near the terminus and inland, with satellite data detecting changes up to 60 km inland, while GPS data capture changes up to 190 km inland along the glacier center line. We attribute this summer speedup to variations in subglacial hydrology, where surface meltwater runoff influences basal friction over the melt season. Incorporating subglacial hydrology into numerical models makes it possible to replicate observed ice velocity patterns.

Plain Language Summary The Northeast Greenland Ice Stream (NEGIS), a crucial part of the Greenland Ice Sheet, has been experiencing significant dynamic thinning recently. This study focuses on the summer speedup of Zachariae Isstrøm (ZI), one of NEGIS's outlet glaciers, which is rapidly retreating and accelerating, highlighting its sensitivity to climate change. Utilizing Sentinel-1 satellite data, in-situ GPS observations, and numerical ice flow modeling, we explore the mechanisms behind short-term dynamic changes. We find that satellite data reveals short-term summer (June to August) fluctuations in ice flow speed near the glacier terminus and up to 50–70 km inland. However, GPS data shows that this speedup extends further inland, up to at least 190 km along the main flow line. Only GPS data can detect the smaller-scale summer speedups in these inland regions, providing critical observations for validating ice flow models. We determine that the seasonal acceleration of ice velocity at Zachariae Isstrøm is due to variations in subglacial hydrology, where surface meltwater runoff reduces basal friction by altering the subglacial hydrologic system during the melt season. Additionally, our study highlights that these findings are applicable beyond NEGIS, with similar speedup patterns observed in other Greenland glaciers.

1. Introduction

The Northeast Greenland Ice Stream (NEGIS), which extends more than 600 km into the interior of the ice sheet, is undergoing sustained dynamic thinning after more than a quarter of a century of stability (Khan et al., 2014; Mouginot et al., 2015). NEGIS drains about 12% of the Greenland Ice Sheet through its three main outlets, Nioghalvfjerdsfjorden Glacier (NG), Zachariae Isstrøm (ZI), and Storstrømmen Glacier (SG) (Mouginot et al., 2015). Recent studies have shown that Zachariæ Isstrøm has experienced rapid retreat and acceleration, with its ice shelf area decreasing by 95% between 2002 and 2014 (Mouginot et al., 2015). This retreat, coupled with increased flow rates and accelerated thinning, highlights the vulnerability of marine-terminating glaciers in this region to changing climate conditions. Factors such as warmer air and ocean temperatures, together with bed topography, have been implicated in driving these dramatic changes (An et al., 2021; Aschwanden et al., 2019; Beckmann & Winkelmann, 2023; Choi et al., 2021; Felikson et al., 2017; Mouginot et al., 2015; Ultee et al., 2022; Wood et al., 2021).

Validation: Shfaqat A. Khan, Eric Rignot, Angelika Humbert, Derek Pickell, Javed Hassan
Visualization: Shfaqat A. Khan
Writing – original draft: Shfaqat A. Khan, Mathieu Morlighem, Shivani Ehrenfeucht, Helene Seroussi, Youngmin Choi, Eric Rignot, Derek Pickell, Javed Hassan

Observing and understanding short-term fluctuations in ice flow speed in Greenland is essential to correctly estimating long-term trends that are used to reduce uncertainty in projections of future ice mass loss trends (Halas et al., 2023; Hanna et al., 2024; Solgaard et al., 2022). Recent studies have used various observational techniques to investigate these dynamic changes. For instance, Hvidberg et al. (2020) employed a GPS network to assess surface velocity on NEGIS, revealing flow patterns and highlighting the importance of accurate velocity measurements for understanding ice stream behavior (Grinsted et al., 2022).

Increasingly, subglacial hydrology has emerged as an important factor influencing ice flow dynamics (Andersen et al., 2023). Subglacial drainage events along NEGIS have been observed to impact ice flow rates, with differential satellite synthetic aperture radar interferometry (DInSAR) providing insights into the spatiotemporal characteristics of these events (Andersen et al., 2023). Moreover, the role of seasonal changes in subglacial hydrology in driving glacier acceleration has been demonstrated by several studies (Davison et al., 2020; Ehrenfeucht et al., 2023; Felikson et al., 2022; Ing et al., 2024; Moon et al., 2014; Price et al., 2008). Additionally, *King et al.* (2018) emphasized the importance of higher-resolution records to capture the temporal response of glaciers to climatic and mechanical drivers, highlighting the need for continuous monitoring to fully understand ice discharge dynamics and its intra-annual variability.

Understanding the variability in seasonal ice flow patterns across the Greenland ice sheet is critical. Vijay et al. (2021) conducted a GrIS-wide glacier classification based on seasonal velocity patterns, revealing distinct behaviors influenced by subglacial hydrology and meltwater dynamics (Ahlstrom et al., 2013; Bartholomew et al., 2011; Moon et al., 2015). Type-1 glacier velocity variations are associated with changes in the ice front position, while type-2 and type-3 seasonal behaviors are related to seasonal shifts in the drainage networks. Type-2 glaciers experience a significant acceleration for a few weeks following the onset of surface melting, after which they slow down to nearly their pre-melt velocities for the remainder of the melt season (Vijay et al., 2021). While satellite-based ice flow maps can detect short-term (weekly) fluctuations in flow speed near the terminus and about 50–70 km inland, changes farther inland are more challenging to detect due to the high signal-to-noise ratio in slow moving regions. To overcome this problem, we use in-situ GPS observations on NEGIS between 80 and 190 km upstream of ZI to detect seasonal changes in flow speed. GPS based flow speed has an accuracy 100 times better than satellite-based observations (Khan et al., 2022) and is therefore an excellent method for detecting small-scale fluctuations. Here, we use a combination of GPS observations and satellite-based ice flow maps on NEGIS to compare with numerical ice flow models and, in particular, study the importance of subglacial hydrology on ice flow speed and its impact on long-term mass changes.

2. Data and Methods

2.1. Ice Speed From GPS and Sentinel-1

We processed the GPS data using the GIPSY-OASIS version 6.4 software Package with high-precision kinematic data processing methods (Christmann et al., 2021; Løkkegaard et al., 2024; Neckel et al., 2020) with ambiguity resolution using Jet Propulsion Laboratory (JPL)'s orbit and clock products (Bertiger et al., 2020). We use JPL's final orbit products, which include satellite orbits, satellite clock parameters, and Earth orientation parameters. The orbit products take the satellite antenna phase center offsets into account. The atmospheric delay parameters are modeled using the Vienna Mapping Function 1 (VMF1) with VMF1grid nominals (Boehm et al., 2006). Corrections are applied to remove the solid Earth tide and ocean tidal loading. The amplitudes and phases of the main ocean tidal loading terms are calculated using the Automatic Loading Provider (https://barre.oso.chalmers.se/loading/l.php) applied to the FES2014b ocean tide model including correction for the center of mass motion of the Earth due to the ocean tides. The site coordinates are computed in the IGS14 frame (Altamimi et al., 2016).

2.2. Surface Speed and Acceleration From Mosaics Based on ESA Sentinel-1 SAR Offset Tracking

We derive ice speeds from mosaics based on ESA Sentinel-1 SAR offset tracking obtained from https://dataverse.geus.dk/dataverse/Ice_velocity. The ice velocity maps of the NEGIS are derived from the intensity tracking of the ESA Sentinel-1 data with a 12-day repeat; and apply the operational IPP chain for the analysis (Solgaard et al., 2021). We use all available ice speed mosaics (provided on a grid with a spatial resolution of 500 m) and associated standard deviations of the underlying shift maps generated by the offset tracking to create a time series of speed for each grid point.

19448007, 2024, 18, Downloaded from https://agupubs.onlinelibrary.wiley.com/doi/10.1029/2024GL110691, Wiley Online Library on [23/10/2024]. See the Terms and Conditions (https://onlinelibrary.wiley.com/terms-and-conditions) on Wiley Online Library for rules of use; OA articles are governed by the applicable Creative Commons License

2.3. Numerical Ice Flow Model

To investigate whether seasonal changes in subglacial hydrology can explain the observed summer speedups on NEGIS, we employ asynchronous coupling between a numerical ice flow model and a subglacial hydrology model to simulate the evolution of effective pressure at the bed during the summer season. In our coupling configuration, evolving effective pressure, the difference between ice overburden pressure and basal water pressure, is used to calculate ice dynamics in a transient simulation, but the evolving ice dynamics do not feed back into calculations of effective pressure. We use the finite element Ice-sheet and Sea-level System Model (ISSM) (Larour et al., 2012) to model the NEGIS and its coupled ice flow-hydrology capability. The horizontal mesh resolution ranges from 200 m near the ice front to 25 km inland, and we apply the Shelfy-Stream Approximation (MacAyeal, 1989) of the stress balance equations for ice flow. We use the surface and bed geometry from BedMachine Greenland v4 (Morlighem et al., 2017) and determine ice viscosity parameters for floating ice and basal friction under grounded ice through inversions.

To establish initial basal conditions, we use the Glacier Drainage System model (GlaDS) to simulate steady-state, winter conditions forced by grounded ice basal melt rates modeled using the same setup as the ISSM contribution to ISMIP6 (Goelzer et al., 2020). GlaDS, a two-dimensional subglacial hydrology model implemented within ISSM, integrates equations for R-channel development and the distribution of meltwater within a sheet-like drainage system, formulated using the empirical Darcy-Weisbach law (Werder et al., 2013). It calculates effective pressure at the glacier base and hydraulic potential across the domain based on meltwater input to a predetermined ice-bedrock geometry. The steady-state conditions of the basal environment are computed without any input from the surface, such that basal melt rates are the only model forcing.

To initialize the ice dynamics model, we apply a regularized Coulomb friction law (Gagliardini, 2007; Schoof, 2005) and invert for the friction coefficient using surface velocities from 2007 to 2008 (Joughin et al., 2017) and steady-state effective pressure results from GlaDS. Transient ice dynamics are highly sensitive to the choice of friction law (Brondex et al., 2017; Choi et al., 2023). Regularized Coulomb friction laws have been shown to reproduce observations well for other Greenland glaciers (Åkesson et al., 2021) as well as for NEGIS specifically (Khan et al., 2022). We choose to use the Schoof friction law (Gagliardini, 2007; Schoof, 2005) specifically because it has been successfully used in previous GlaDS-ISSM coupled model studies (Ehrenfeucht et al., 2023; Pelle et al., 2024).

We allow the ice dynamics modules a 20-year relaxation period before turning on coupling between subglacial hydrology and ice dynamics to decrease the computational intensity of model spinup. During this time, steady-state effective pressure is used to calculate ice flow under constant atmospheric and oceanic forcing. We then run an additional 5-year model relaxation with synchronous coupling between ISSM and GlaDS, where outputs from both models are able to influence the other. The final output of the coupled relaxation period is used as initial conditions for our experimental model simulations.

We model the subglacial hydrologic system and ice flow dynamics of NEGIS over a 10 year period, from 2008 to 2018, using asynchronous coupling between transient simulations. We first run GlaDS without updating ice geometry or velocity over NEGIS from 2008 to 2018 using the final state from the synchronously coupled relaxation simulation to initialize the transient subglacial hydrology model. We use an adaptive timestep satisfying the CFL condition and ranging from 10 min to 1 day depending on the maximum water velocity through the subglacial environment. In addition to steady-state basal melt, GlaDS is forced using daily surface melt water runoff from the Modèle Atmosphérique Régional (MARv3.10; Fettweis et al., 2017; Tedesco & Fettweis, 2020). Limited information is available about the number and locations of moulins in this region. Given the lack of readily accessible data, we insert meltwater runoff directly to the bed without making additional assumptions about water routing through a supraglacial hydrologic system or being funneled to the bed at discrete locations.

In order to assess the impact of changes in effective pressure during the melt season on ice flow dynamics, we use the resulting time-series of evolving effective pressure as a transient forcing in the ice flow model spanning the same time period of 2008–2018. The ice flow model is additionally forced with observed weekly ice front positions from LandSat-8 (https://www.usgs.gov/landsat-missions/landsat-8) (Wood et al., 2021), and with daily surface mass balance from MAR (Tedesco & Fettweis, 2020). We use the same basal melt parameterization from (Choi et al., 2021) to represent ocean-driven melting under floating ice (see in Supporting Information S1 for additional details).

19448007, 2024, 18, Downloaded from https://agupubs.onlinelibrary.wiley.com/doi/10.1029/2024GL110691, Wiley Online Library on [23/10/2024]. See the Terms and Conditions (https://onlinelibrary.wiley.com/terms-and-conditions) on Wiley Online Library for rules of use; OA articles are governed by the applicable Creative Commons License

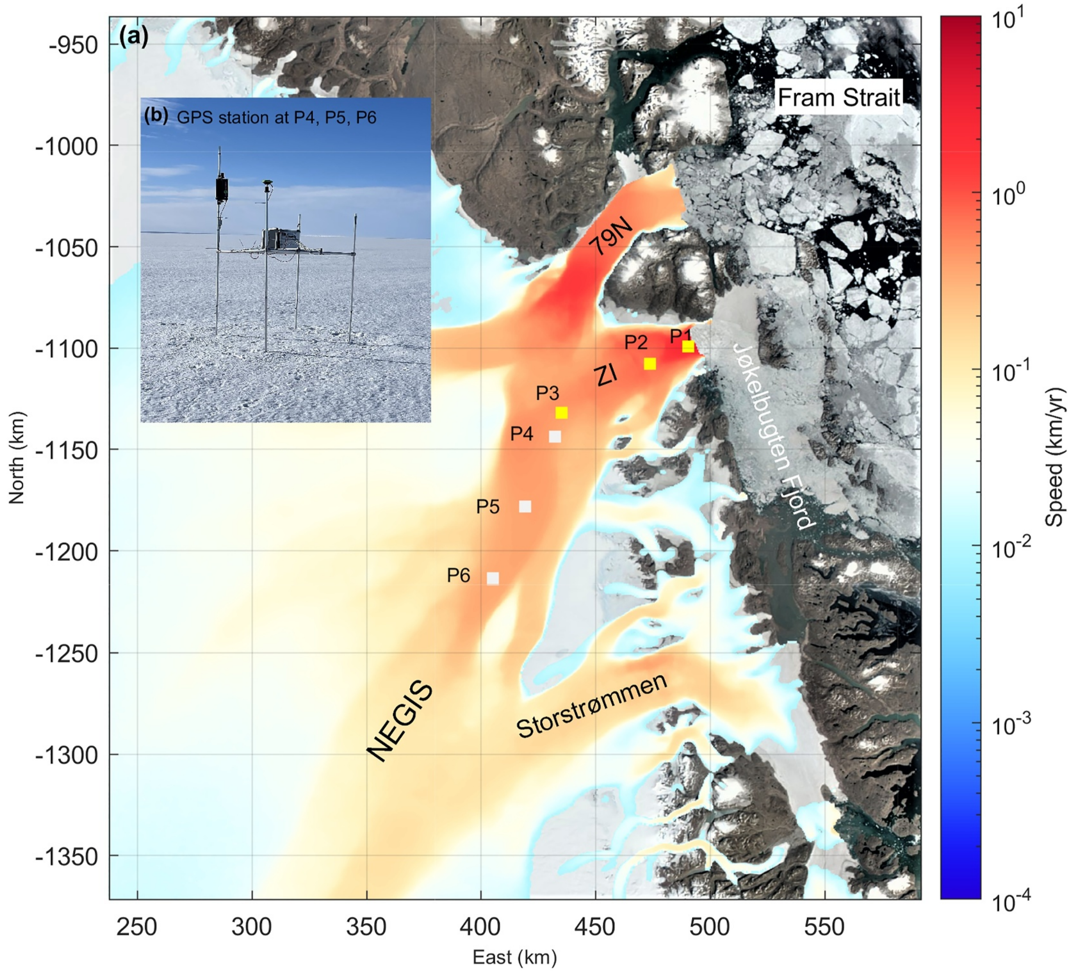

Figure 1. (a) Satellite-derived surface speed from 2007. A Landsat-8 image from 2017 is used as the background. The locations of GNSS stations, P4, P5, P6 are marked by gray boxes. P1, P2, P3 are selected points (yellow boxes) where we estimate ice flow time series using ESA Sentinel-1 data. (b) Photo of the P6 station setup, which consists of an antenna, a receiver, and a solar panel (source and permission: Shfaqat Abbas Khan). All stations are situated on a platform about 1.7 m above the ice surface.

3. Results

The velocity time series of ice flow at points P1 to P3 (Figure 1a) is estimated utilizing data from ESA's Sentinel-1 satellite, which offers a 12-day revisit interval (Figure 2a). Conversely, for points P4 to P6, we rely on GPS data to derive the ice flow velocity time series. The GPS-derived ice speed at points P4 to P6 exhibits an uncertainty of approximately 0.03 m/yr, while the satellite-derived ice speed carries an uncertainty of about 3 m/yr. Our modeled winter ice flow velocity time series with and without subglacial hydrology (Figures 2b and 2c) align with observations. Both the observed and modeled winter velocity profiles indicate a gradual decrease in speed inland along the main flow line. Notably, Figure 2b presents the modeled velocity incorporating subglacial hydrology, whereas Figure 2c excludes this factor. It is noteworthy that the modeled velocity without subglacial hydrology fails to replicate the summer speedup observed by ESA's Sentinel-1 satellite and GPS data.

To focus on the magnitude of the summer speedup, we compare relative ice speed (Figure 3) rather than absolute ice speed (Figure 2). For each time series, we subtract the minimum speed during 2017 to obtain the magnitude of the summer speedup. Ice speeds from Sentinel-1 suggest an increase in speed of 630.8 ± 15.1 m/yr at P1, 360.2 ± 10.0 m/yr at P2, and 107.5 ± 10.9 m/yr at P3; however, no significant speedup is observed at P4 (19.1 ± 20.8). Hence, ice speed from satellite data suggests the summer speedup propagated up to approximately 60 km inland from the terminus and along the main flowline.

19448007, 2024, 18, Downloaded from https://agupubs.onlinelibrary.wiley.com/doi/10.1029/2024GL110691, Wiley Online Library on [23/10/2024]. See the Terms and Conditions (https://onlinelibrary.wiley.com/terms-and-conditions) on Wiley Online Library for rules of use; OA articles are governed by the applicable Creative Commons License

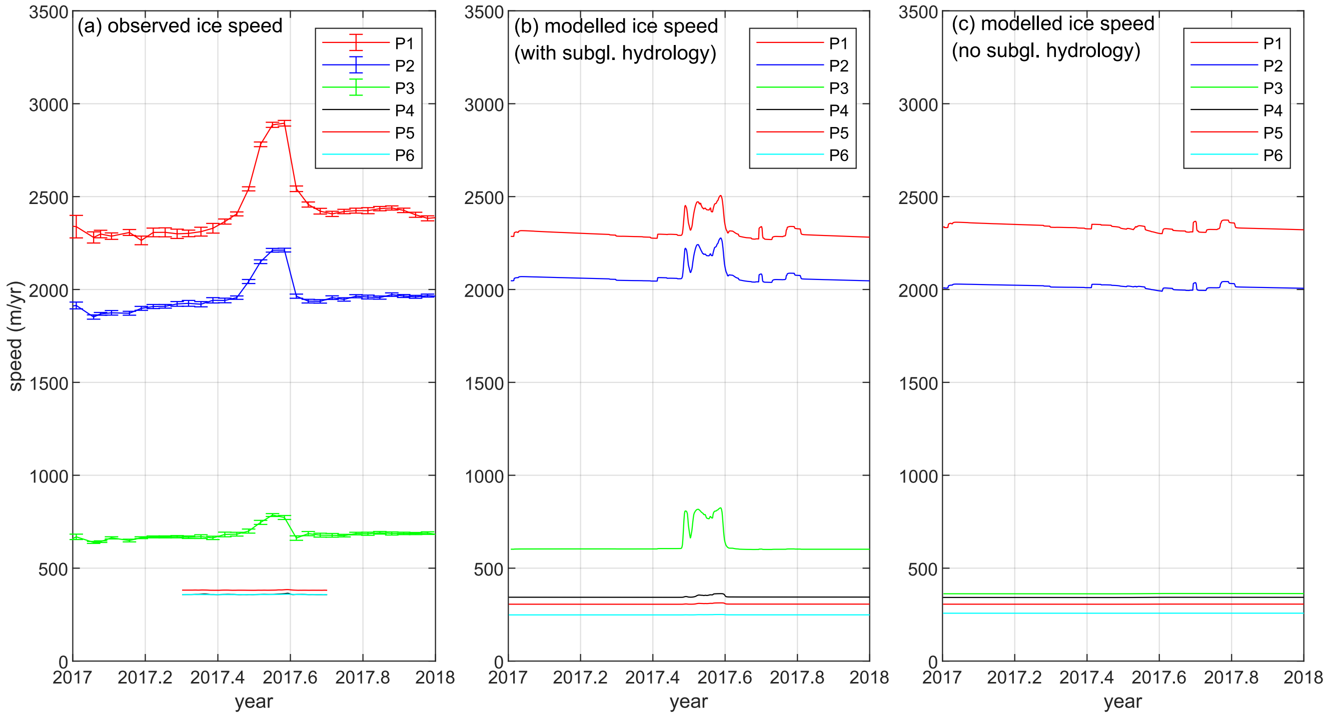

Figure 2. (a) Time series of observed flow speed at P1 to P3 using ESA's Sentinel-1 satellite data with observed uncertainties, and observed flow speed using GPS data at P4 to P6. (b) Modeled ice speed using numerical flow models that include a subglacial hydrology model. (c) Modeled ice speed using numerical flow models without coupling to subglacial hydrology.

The points P4 to P6 are located between 80 and 190 km inland. Here, we estimate relative ice speed using GPS data. Figure 3d shows summer speedup detected by GPS at P4 to P6. The magnitude of the summer speedup declines from 7.16 ± 0.03 m/yr at P4 to 3.88 ± 0.03 m/yr at P5 and to 2.24 ± 0.03 m/yr at P6. Figures 3b and 3e show modeled relative speedup including subglacial hydrology, while Figures 3c and 3f show modeled results without subglacial hydrology. The large amplitude of summer speedups observed near the terminus using satellite data and deep inland using GPS data can only be reproduced by an ice flow model that has subglacial hydrology incorporated.

4. Discussion

Flow velocity maps derived from Sentinel-1 SAR offset tracking have proven effective in capturing short-term speedups near glacier termini and up to approximately 60 km inland. However, the precision of this method limits its capability to detect smaller changes further inland. Notably, long-term changes (>3 years) can be discerned using Sentinel-1 data (Khan et al., 2022). Our modeled background winter speeds, both with and without consideration of subglacial hydrology, generally aligns well with observed speeds from GPS and Sentinel-1. While studies focusing on long-term changes often compare modeled velocity with mean annual velocity or winter velocities, thereby potentially overlooking short-term summer fluctuations, these short-term variations may play a crucial role in enhancing our understanding of long-term changes in glacier speed, mass change, and dynamic thinning.

The long-term trend in ice velocity at ZI is controlled by the migration of the ice front (Khan et al., 2022), but the migration of the ice front cannot explain the short-term seasonal changes in ice speed. In this study, we investigate another physical process, hydrology, to explain these short-term changes. Additionally, detecting short-term inland speedups beyond 80 km has been challenging without in-situ GPS measurements, making it difficult to monitor inland summer speedups of the ZI until now. With the availability of new, accurate GPS data, we reassess the role of subglacial hydrology in glacier flow speed. Our modeling study indicates that subglacial hydrology is the main mechanism responsible for the small but detectable speedups observed by GPS between 90 and 190 km

RIGHTSLINK Copyright Clearance Center

19448007, 2024, 18, Downloaded from https://agupubs.onlinelibrary.wiley.com/doi/10.1029/2024GL110691, Wiley Online Library on [23/10/2024]. See the Terms and Conditions (https://onlinelibrary.wiley.com/terms-and-conditions) on Wiley Online Library for rules of use; OA articles are governed by the applicable Creative Commons License

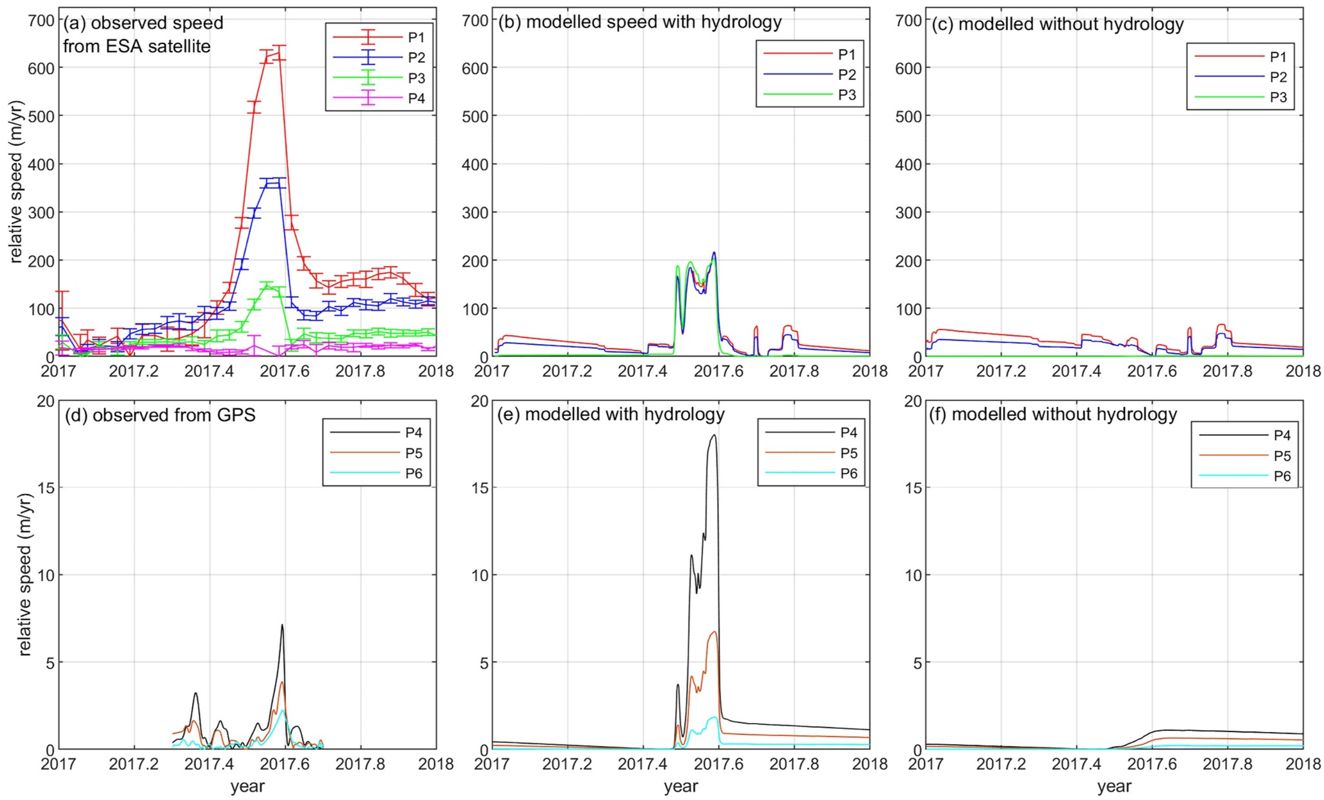

Figure 3. (a) Relative flow speed using ESA's Sentinel-1 satellite data at P1 to P4. (b) Modeled relative ice speed at P1 to P3 using numerical flow models that include a subglacial hydrology model. (c) Modeled relative ice speed at P1 to P3 using numerical flow models excluding subglacial hydrology. (d) Relative flow speed using GPS data at P4 to P6. (e) same as (b) for P4 to P6. (f) Same as (c) for P4 to P6.

inland. Furthermore, our modeling suggests that subglacial hydrology could potentially be the primary cause of the seasonal speedup at the glacier front.

The retreat of the glacier terminus induces only minor fluctuations far from the terminus (see Figure 3c). Although our numerical flow model that includes the effect of subglacial hydrology better fits observed speed fluctuations near the terminus and inland, it deviates from observations by a factor of 2–3 (see Table 1). Specifically, the model underestimates the summer speedup by a factor of 2–3 at P1 and P2 and overestimates the speedup by approximately 2 at P3 to P5. P6 exhibits the best agreement between model and observation. The region encompassing P1 and P2 is characterized by a rapid drop in ice surface and bed elevation compared to P3-P5 (Figures 4a and 4b). This complex glacier geometry poses a challenge for the subglacial hydrology model, as it is difficult to precisely model the entry points of summer meltwater runoff into the subglacial hydrological system through cracks and moulins at the ice surface. It is likely that summer meltwater runoff in the region of P3-P5 travels through extensive surface meltwater channels and enters the bed closer to the region of P1-P2, likely near the drop in ice surface elevation (indicated as a dashed red line in Figure 4b). The magnitude of speedup in response to seasonal meltwater runoff is also likely skewed in our model results due to the offline coupling between subglacial hydrology and ice dynamics in our transient simulations. An increase in velocity will increase the cavity opening rate in the basal environment, leading to faster transport of meltwater through the subglacial hydraulic system which moderates how large water pressure is able to grow (Hoffman & Price, 2014). In our transient simulations, the cavity opening rate remains constant throughout the melt season, likely leading to an over-estimate of water pressures. Coupling between subglacial hydrology and ice flow models is a somewhat new advance in modeling capabilities. The relative impact of coupling between different parameters remains unknown,

Table 1
Observed and Modeled Magnitude of the 2017 Summer Speedup

Site	Observed speed (m/yr)	Model with hydrology (m/yr)
P1	630.8 ± 15.1 (Sentinel-1)	217.1
P2	360.2 ± 10.0 (Sentinel-1)	205.7
P3	107.5 ± 10.9 (Sentinel-1)	203.8
P4	7.16 ± 0.03 (GPS)	17.9
P5	3.88 ± 0.03 (GPS)	6.6
P6	2.11 ± 0.03 (GPS)	1.8

19448007, 2024, 18, Downloaded from https://agupubs.onlinelibrary.wiley.com/doi/10.1029/2024GL110691, Wiley Online Library on [23/10/2024]. See the Terms and Conditions (https://onlinelibrary.wiley.com/terms-and-conditions) on Wiley Online Library for rules of use; OA articles are governed by the applicable Creative Commons License

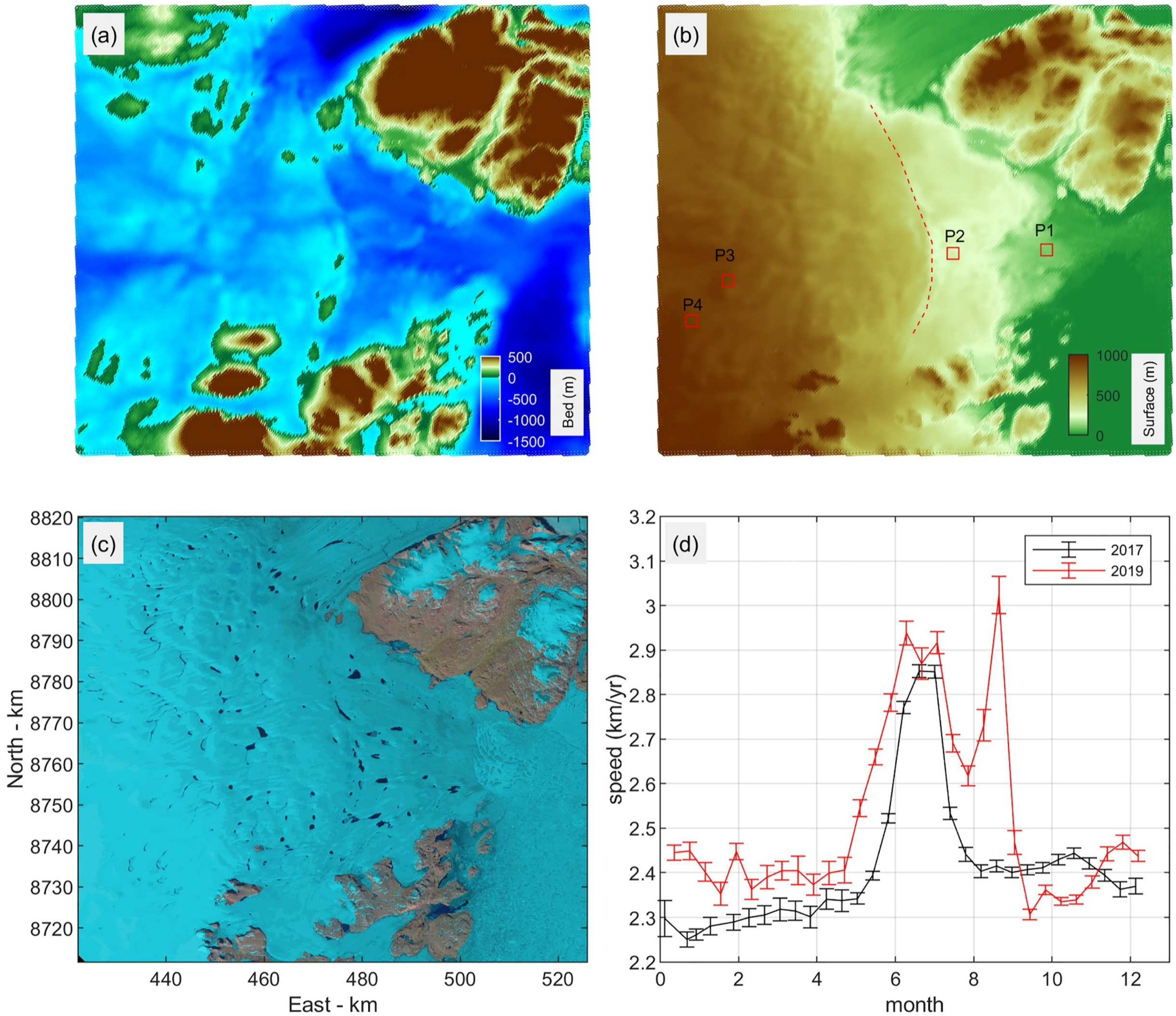

Figure 4. (a) Bed topography and (b) surface topography from BedMachine Greenland v4 ((Morlighem et al., 2017). The red squares in (b) denote locations of P1 to P4. The red dashed line denotes an area with sharp decline in elevation. (c) Landsat image conducted on 20 July 2017 showing meltwater lakes (dark spots) on ZI. (d) Time series of surface speed at point P1 in 2017 and 2019.

but is of interest for future work. The response of the model is also strongly controlled by the choice of friction law, which remains an area of active research (Choi et al., 2023).

The total modeled mass loss of the NEGIS during 2017 is 16.1 Gt for a flow model that does not include subglacial hydrology. The summer speedup of 630 m/yr at P1 increases ice discharge and the associated ice loss by an additional 1.5 Gt/yr (due to increased ice discharge through a flux gate at the grounding line). This 10% increase in ice loss due to subglacial hydrology is critical and must be incorporated into flow models, as future warming is expected to lead to enhanced melting during summer periods (Beckmann & Winkelmann, 2023). Additionally, summers are predicted to last longer with more extreme melt events on the ice sheet (Beckmann & Winkelmann, 2023), resulting in longer periods with increased surface meltwater runoff into the subglacial hydrological system. Over the past decade, the Greenland Ice Sheet experienced record-high mass loss in 2012 (Bevis et al., 2019), followed by an even larger mass loss in 2019 (Sasgen et al., 2020; Velicogna et al., 2020). Figure 4d illustrates the summer speedup at P1 in 2017 and during the exceptionally high record mass loss year of 2019. The 2019 speedup was more intense, started earlier, and ended later compared to the 2017 summer speedup. In a warmer climate, longer periods of increased melt may result in an increase in ice loss at the NEGIS. However, seasonal fluctuations in ocean, atmosphere and terminus position have a complex effect on long term mass loss, for example, Felikson et al. (2022) showed that leaving out seasonal signal can cause either an overestimate or

19448007, 2024, 18, Downloaded from https://agupubs.onlinelibrary.wiley.com/doi/10.1029/2024GL110691, Wiley Online Library on [23/10/2024]. See the Terms and Conditions (https://onlinelibrary.wiley.com/terms-and-conditions) on Wiley Online Library for rules of use; OA articles are governed by the applicable Creative Commons License

RIGHTSLINK

underestimate of long term mass loss, depending on the slope of the bed and the amount of seasonal terminus movement.

Several glacier systems in Greenland with large drainage basins (e.g., Petermann Glacier in northeast Greenland and Jakobshavn Isbræ in central west Greenland) exhibit speedup patterns similar to those observed at ZI (Løkkegaard et al., 2024; Millan et al., 2022; Moon et al., 2014). The peak velocity of these type-2 glaciers occurs during the melt season, in contrast to type-3 glaciers, where the peak velocity occurs prior to the melt season (Vijay et al., 2021). Out of 221 glaciers, 48 exhibit type-2 behavior and could potentially experience enhanced ice loss in the future, as the melt season lengthens.

In recent decades, the ablation area in north Greenland expanded to higher elevations and increased by 46%, which is twice as much as in the south (+25%) (Noël et al., 2019). To accurately model the small accelerations at higher elevations (often in order of few m/yr^2 (Khan et al., 2022)), high-precision in-situ GPS data as used here or an improved processing strategy for satellite-based velocity maps is required (Andersen et al., 2023).

5. Conclusions

We presented new insights concerning seasonal dynamic changes occurring within the Northeast Greenland Ice Stream and underscore the vulnerability of marine-terminating glaciers in this region to evolving climate conditions. Through a combination of observational techniques and numerical modeling, we elucidate the complex interplay of factors driving ice flow dynamics, particularly focusing on the role of subglacial hydrology. By accurately measuring the observed ice velocity from satellite data, we detect short-term summer (June to August) fluctuations in flow speed near the terminus and up to about 50–70 km inland. Furthermore, our in-situ GPS data suggest the short-term speedup migrates further inland, to at least 190 km along the main flow line. In this inland region of NEGIS, only GPS data can detect the small-scale amplitude of summer speedup and thereby provide crucial observations for ice flow model validation. We ascertain that the short-term seasonal acceleration of ice velocity on Zachariæ Isstrøm can be attributed to variations in subglacial hydrology based on results form asynchronous coupling between subglacial hydrology and ice flow models, wherein surface meltwater runoff mitigates basal friction through the evolution of the subglacial hydrologic system over the melt season. Moreover, our study underscores the broader relevance of these findings beyond NEGIS, with similar speedup patterns observed in other glacier systems across Greenland. As climate warming continues to exert pressure on the Greenland Ice Sheet, understanding and accurately modeling these dynamic processes are essential for accurately predicting future ice loss and its implications for global sea-level rise.

Data Availability Statement

BedMachine Greenland is available from the National Snow and Ice Data Center (NSIDC) (Morlighem et al., 2022). MAR SMB and runoff information can be found accessed at http://ftp.climato.be/fettweis/MARv3.10/Greenland/ERA5_1950-2021-6km/ (Tedesco & Fettweis, 2020). The ice fronts time series is available at Wood et al. (2020). Ocean thermal forcing data are available at Wood et al. (2020). The ice speed obtained from mosaics based on ESA Sentinel-1 SAR offset tracking are available at A. Solgaard & Kusk (2024). GPS time series of ice speed is available at Khan (2024). The ISSM is open source and is available at http://issm.jpl.nasa.gov (Version 4.24, released on 26 May 2024).

Acknowledgments
S.A.K. acknowledge support from the Carlsberg Foundation—Semper Ardens Advance program (Grant CF22-0628). We thank the editor (Dr. Minghua Zhang), and reviewers, Dr. Lizz Ultee, Dr. Amy Jenson, and an anonymous reviewer for their insightful and constructive comments to earlier drafts of this manuscript.

References

Ahlstrøm, A. P., Andersen, S. B., Andersen, M. L., Machguth, H., Nick, F. M., Joughin, I., et al., (2013). Seasonal velocities of eight major marine-terminating outlet glaciers of the Greenland ice sheet from continuous in situ GPS instruments. *Earth System Science Data*, *5*(2), 277–287. https://doi.org/10.5194/essd-5-277-2013

Åkesson, H., Morlighem, M., O'Regan, M., & Jakobsson, M. (2021). Future projections of Petermann Glacier under ocean warming depend strongly on friction law. *Journal of Geophysical Research: Earth Surface*, *126*(6), e2020JF005921. https://doi.org/10.1029/2020JF005921

Altamimi, Z., Rebischung, P., Métivier, L., & Collilieux, X. (2016). ITRF2014: A new release of the international terrestrial reference frame modeling nonlinear station motions. *Journal of Geophysical Research: Solid Earth*, *121*(8), 6109–6131. https://doi.org/10.1002/2016JB013098

An, L., Rignot, E., Wood, M., Willis, J. K., Mouginot, J., & Khan, S. A. (2021). Ocean melting of the Zachariae Isstrøm and Nioghalvfjerdsfjorden glaciers, northeast Greenland. *Proceedings of the National Academy of Sciences*, *118*(2), e2015483118. https://doi.org/10.1073/pnas.2015483118

Andersen, J. K., Rathmann, N., Hvidberg, C. S., Grinsted, A., Kusk, A., Merryman Boncori, J. P., & Mouginot, J. (2023). Episodic subglacial drainage cascades below the Northeast Greenland ice stream. *Geophysical Research Letters*, *50*(12), e2023GL103240. https://doi.org/10.1029/2023GL103240

19448007, 2024, 18, Downloaded from https://agupubs.onlinelibrary.wiley.com/doi/10.1029/2024GL110691, Wiley Online Library on [23/10/2024]. See the Terms and Conditions (https://onlinelibrary.wiley.com/terms-and-conditions) on Wiley Online Library for rules of use; OA articles are governed by the applicable Creative Commons License

19448007, 2024, 18, Downloaded from https://agupubs.onlinelibrary.wiley.com/doi/10.1029/2024GL110691, Wiley Online Library on [23/10/2024]. See the Terms and Conditions (https://onlinelibrary.wiley.com/terms-and-conditions) on Wiley Online Library for rules of use; OA articles are governed by the applicable Creative Commons License

Aschwanden, A., Fahnestock, M. A., Truffer, M., Brinkerhoff, D. J., Hock, R., Khroulev, C., et al. (2019). Contribution of the Greenland Ice Sheet to sea level over the next millennium. *Science Advances*, *5*(6), eaav9396. https://doi.org/10.1126/sciadv.aav9396

Bartholomew, I., Nienow, P., Sole, A., Mair, D., Cowton, T., Palmer, S., & Wadham, J. (2011). Supraglacial forcing of subglacial drainage in the ablation zone of the Greenland ice sheet. *Geophysical Research Letters*, *38*(8), L08502. https://doi.org/10.1029/2011GL047063

Beckmann, J., & Winkelmann, R. (2023). Effects of extreme melt events on ice flow and sea level rise of the Greenland Ice Sheet. *The Cryosphere*, *17*(7), 3083–3099. https://doi.org/10.5194/tc-17-3083-2023

Bertiger, W., Bar-Sever, Y., Dorsey, A., Haines, B., Harvey, N., Hemberger, D., et al. (2020). GipsyX/RTGx, a new tool set for space geodetic operations and research. *Advances in Space Research*, *66*(3), 469–489. https://doi.org/10.1016/j.asr.2020.04.015

Bevis, M., Harig, C., Khan, S. A., Brown, A., Simons, F. J., Willis, M., et al. (2019). Accelerating changes in ice mass within Greenland, and the ice sheet's sensitivity to atmospheric forcing. *Proceedings of the National Academy of Sciences*, *116*(6), 1934–1939. https://doi.org/10.1073/pnas.1806562116

Boehm, J., Werl, B., & Schuh, H. (2006). Troposphere mapping functions for GPS and very long baseline interferometry from European Centre for Medium-Range Weather Forecasts operational analysis data. *Journal of Geophysical Research*, *111*(B2). https://doi.org/10.1029/2005JB003629

Brondex, J., Gagliardini, O., Gillet-Chaulet, F., & Durand, G. (2017). Sensitivity of grounding line dynamics to the choice of the friction law. *Journal of Glaciology*, *63*(241), 854–866. https://doi.org/10.1017/jog.2017.51

Choi, Y., Morlighem, M., Rignot, E., & Wood, M. (2021). Ice dynamics will remain a primary driver of Greenland ice sheet mass loss over the next century. *Communications Earth & Environment*, *2*(1), 26. https://doi.org/10.1038/s43247-021-00092-z

Choi, Y., Seroussi, H., Morlighem, M., Schlegel, N. J., & Gardner, A. (2023). Impact of time-dependent data assimilation on ice flow model initialization and projections: A case study of Kjer glacier, Greenland. *The Cryosphere*, *17*(12), 5499–5517. https://doi.org/10.5194/tc-17-5499-2023

Christmann, J., Helm, V., Khan, S. A., Kleiner, T., Müller, R., Morlighem, M., et al. (2021). Elastic deformation plays a non-negligible role in Greenland's outlet glacier flow. *Communications Earth & Environment*, *2*(1), 232. https://doi.org/10.1038/s43247-021-00296-3

Davison, B. J., Sole, A. J., Cowton, T. R., Lea, J. M., Slater, D. A., Fahrner, D., & Nienow, P. W. (2020). Subglacial drainage evolution modulates seasonal ice flow variability of three tidewater glaciers in southwest Greenland. *Journal of Geophysical Research: Earth Surface*, *125*(9), e2019JF005492. https://doi.org/10.1029/2019JF005492

Ehrenfeucht, S., Morlighem, M., Rignot, E., Dow, C. F., & Mouginot, J. (2023). Seasonal acceleration of Petermann Glacier, Greenland, from changes in subglacial hydrology. *Geophysical Research Letters*, *50*(1), e2022GL098009. https://doi.org/10.1029/2022GL098009

Felikson, D., Bartholomaus, T. C., Catania, G. A., Korsgaard, N. J., Kjær, K. H., Morlighem, M., et al. (2017). Inland thinning on the Greenland ice sheet controlled by outlet glacier geometry. *Nature Geoscience*, *10*(5), 366–369. https://doi.org/10.1038/ngeo2934

Felikson, D., Nowicki, S., Nias, I., Morlighem, M., & Seroussi, H. (2022). Seasonal tidewater glacier terminus oscillations bias multi-decadal projections of ice mass change. *Journal of Geophysical Research: Earth Surface*, *127*(2), e2021JF006249. https://doi.org/10.1029/2021JF006249

Fettweis, X., Box, J. E., Agosta, C., Amory, C., Kittel, C., Lang, C., et al. (2017). Reconstructions of the 1900–2015 Greenland ice sheet surface mass balance using the regional climate MAR model. *The Cryosphere*, *11*(2), 1015–1033. https://doi.org/10.5194/tc-11-1015-2017

Gagliardini, O., Cohen, D., Råback, P., & Zwinger, T. (2007). Finite-element modeling of subglacial cavities and related friction law. *Journal of Geophysical Research*, *112*(F2). https://doi.org/10.1029/2006JF000576

Goelzer, H., Nowicki, S., Payne, A., Larour, E., Seroussi, H., Lipscomb, W. H., et al. (2020). The future sea-level contribution of the Greenland ice sheet: A multi-model ensemble study of ISMIP6. *The Cryosphere*, *14*(9), 3071–3096. https://doi.org/10.5194/tc-14-3071-2020

Grinsted, A., Hvidberg, C. S., Lilien, D. A., Rathmann, N. M., Karlsson, N. B., Gerber, T., et al. (2022). Accelerating ice flow at the onset of the Northeast Greenland ice stream. *Nature Communications*, *13*(1), 5589. https://doi.org/10.1038/s41467-022-32999-2

Halas, P., Mouginot, J., Fleurian, B., & Langebroek, P. M. (2023). Impact of seasonal fluctuations of ice velocity on decadal trends observed in Southwest Greenland. *Remote Sensing of Environment*, *285*, 113419. https://doi.org/10.1016/j.rse.2022.113419

Hanna, E., Topál, D., Box, J. E., Buzzard, S., Christie, F. D. W., Hvidberg, C., et al. (2024). Short- and long-term variability of the Antarctic and Greenland ice sheets. *Nature Reviews Earth and Environment*, *5*(3), 193–210. https://doi.org/10.1038/s43017-023-00509-7

Hoffman, M., & Price, S. (2014). Feedbacks between coupled subglacial hydrology and glacier dynamics. *Journal of Geophysical Research: Earth Surface*, *119*(3), 414–436. https://doi.org/10.1002/2013JF002943

Hvidberg, C. S., Grinsted, A., Dahl-Jensen, D., Khan, S. A., Kusk, A., Andersen, J. K., et al. (2020). Surface velocity of the Northeast Greenland ice stream (NEGIS): Assessment of interior velocities derived from satellite data by GPS. *The Cryosphere*, *14*(10), 3487–3502. https://doi.org/10.5194/tc-14-3487-2020

Ing, R. N., Nienow, P. W., Sole, A. J., Tedstone, A. J., & Mankoff, K. D. (2024). Minimal impact of late-season melt events on Greenland Ice Sheet annual motion. *Geophysical Research Letters*, *51*(4), e2023GL106520. https://doi.org/10.1029/2023GL106520

Joughin, I., Smith, B. E., Howat, I. M., Scambos, T., & Moon, T. (2017). Greenland flow variability from ice-sheet-wide velocity mapping. *Journal of Glaciology*, *56*(197), 415–430. https://doi.org/10.3189/002214310792447734

Khan, S. A. (2024). GPS data from NEGIS, Greenland. [Dataset]. *Zenodo*. https://doi.org/10.5281/zenodo.13451664

Khan, S. A., Choi, Y., Morlighem, M., Rignot, E., Helm, V., Humbert, A., et al. (2022). Extensive inland thinning and speed-up of northeast Greenland ice stream. *Nature*, *611*(7937), 727–732. https://doi.org/10.1038/s41586-022-05301-z

Khan, S. A., Kjær, K. H., Bevis, M., Bamber, J. L., Wahr, J., Kjeldsen, K. K., et al. (2014). Sustained mass loss of the northeast Greenland ice sheet triggered by regional warming. *Nature Climate Change*, *4*(4), 292–299. https://doi.org/10.1038/nclimate2161

King, M. D., Howat, I. M., Jeong, S., Noh, M. J., Wouters, B., Noël, B., & van den Broeke, M. R. (2018). Seasonal to decadal variability in ice discharge from the Greenland Ice Sheet. *The Cryosphere*, *12*(12), 3813–3825. https://doi.org/10.5194/tc-12-3813-2018

Larour, E., Seroussi, H., Morlighem, M., & Rignot, E. (2012). Continental scale, high order, high spatial resolution, ice sheet modeling using the Ice Sheet System Model (ISSM). *Journal of Geophysical Research*, *117*(F1). https://doi.org/10.1029/2011JF002140

Løkkegaard, A., Colgan, W., Hansen, K., Thorsøe, K., Jakobsen, J., & Khan, S. A. (2024). Ice acceleration and rotation in the Greenland Ice Sheet interior in recent decades. *Communications Earth & Environment*, *5*(1), 211. https://doi.org/10.1038/s43247-024-01322-w

MacAyeal, D. R. (1989). Large-scale ice flow over a viscous basal sediment: Theory and application to ice stream B, Antarctica. *Journal of Geophysical Research*, *94*(B4), 4071–4087. https://doi.org/10.1029/JB094iB04p04071

Millan, R., Mouginot, J., Derkacheva, A., Rignot, E., Milillo, P., Ciraci, E., et al. (2022). Ongoing grounding line retreat and fracturing initiated at the Petermann Glacier ice shelf, Greenland, after 2016. *The Cryosphere*, *16*(7), 3021–3031. https://doi.org/10.5194/tc-16-3021-2022

Moon, T., Joughin, I., & Smith, B. (2015). Seasonal to multiyear variability of glacier surface velocity, terminus position, and sea ice/ice mélange in northwest Greenland. *J. Geophys. Res.Earth Surface*, *120*(5), 818–833. https://doi.org/10.1002/2015JF003494

RIGHTSLINK Copyright Clearance Center

19448007, 2024, 18, Downloaded from https://agupubs.onlinelibrary.wiley.com/doi/10.1029/2024GL110691, Wiley Online Library on [23/10/2024]. See the Terms and Conditions (https://onlinelibrary.wiley.com/terms-and-conditions) on Wiley Online Library for rules of use; OA articles are governed by the applicable Creative Commons License

Moon, T., Joughin, I., Smith, B., van den Broeke, M. R., van de Berg, W. J., Noël, B., & Usher, M. (2014). Distinct patterns of seasonal Greenland glacier velocity. *Geophysical Research Letters*, *41*(20), 7209–7216. https://doi.org/10.1002/2014GL061836

Morlighem, M., Williams, C. N., Rignot, E., An, L., Arndt, J. E., Bamber, J. L., et al. (2022). IceBridge BedMachine Greenland, version 5. [Dataset]. NASA National Snow and Ice Data Center Distributed Active Archive Center. https://doi.org/10.5067/GMEVBWFLWA7X

Morlighem, M., Williams, C. N., Rignot, E., An, L., Arndt, J. E., Bamber, J. L., et al. (2017). BedMachine v3: Complete bed topography and ocean bathymetry mapping of Greenland from multibeam echo sounding combined with mass conservation. *Geophysical Research Letters*, *44*(21), 11051–11061. https://doi.org/10.1002/2017GL074954

Mouginot, J., Rignot, E., Scheuchl, B., Fenty, I., Khazendar, A., Morlighem, M., et al. (2015). Fast retreat of Zachariæ Isstrøm, northeast Greenland. *Science*, *350*(6266), 1357–1361. https://doi.org/10.1126/science.aac7111

Neckel, N., Zeising, O., Steinhage, D., Helm, V., & Humbert, A. (2020). Seasonal observations at 79°N glacier (Greenland) from remote sensing and in situ measurements. *Frontiers in Earth Science*, *8*. https://doi.org/10.3389/feart.2020.00142

Noël, B., van de Berg, W. J., Lhermitte, S., & van den Broeke, M. R. (2019). Rapid ablation zone expansion amplifies north Greenland mass loss. *Science Advances*, *5*(9), eaaw0123. https://doi.org/10.1126/sciadv.aaw0123

Pelle, T., Greenbaum, J., Ehrenfeucht, S., Dow, C., & McCormack, F. (2024). Subglacial discharge accelerates dynamic retreat of aurora subglacial basin outlet glaciers, East Antarctica, over the 21st century. *Journal of Geophysical Research: Earth Surface*, *129*(7), e2023JF007513. https://doi.org/10.1029/2023JF007513

Price, S. F., Payne, A. J., Catania, G. A., & Neumann, T. A. (2008). Seasonal acceleration of inland ice via longitudinal coupling to marginal ice. *Journal of Glaciology*, *54*(185), 213–219. https://doi.org/10.3189/002214308784886117

Sasgen, I., Wouters, B., Gardner, A. S., King, M. D., Tedesco, M., Landerer, F. W., et al. (2020). Return to rapid ice loss in Greenland and record loss in 2019 detected by the GRACE-FO satellites. *Communications Earth & Environment*, *1*(1), 8. https://doi.org/10.1038/s43247-020-0010-1

Schoof, C. (2005). The effect of cavitation on glacier sliding. *Proceedings of the Royal Society A: Mathematical, Physical and Engineering Sciences*, *461*(2055), 609–627. https://doi.org/10.1098/rspa.2004.1350

Solgaard, A. M., & Kusk, A. (2024). Greenland ice velocity from Sentinel-1 edition 4. [Dataset]. *GEUS Dataverse*, *19*. https://doi.org/10.22008/FK2/LFZLZN

Solgaard, A. M., Kusk, A., Merryman Boncori, J. P., Dall, J., Mankoff, K. D., Ahlstrøm, A. P., et al. (2021). Greenland ice velocity maps from the PROMICE project. *Earth System Science Data*, *13*(7), 3491–3512. https://doi.org/10.5194/essd-13-3491-2021

Solgaard, A. M., Rapp, D., Noël, B. P. Y., & Hvidberg, C. S. (2022). Seasonal patterns of Greenland ice velocity from Sentinel-1 SAR data linked to runoff. *Geophysical Research Letters*, *49*(24), e2022GL100343. https://doi.org/10.1029/2022GL100343

Tedesco, M., & Fettweis, X. (2020). Unprecedented atmospheric conditions (1948–2019) drive the 2019 exceptional melting season over the Greenland ice sheet. *The Cryosphere*, *14*(4), 1209–1223. https://doi.org/10.5194/tc-14-1209-2020

Ultee, L., Felikson, D., Minchew, B., Stearns, L. A., & Riel, B. (2022). Helheim Glacier ice velocity variability responds to runoff and terminus position change at different timescales. *Nature Communications*, *13*(1), 6022. https://doi.org/10.1038/s41467-022-33292-y

Velicogna, I., Mohajerani, Y., Geruo, A., Landerer, F., Mouginot, J., Noel, B., et al. (2020). Continuity of ice sheet mass loss in Greenland and Antarctica from the GRACE and GRACE follow-on missions. *Geophysical Research Letters*, *47*(8), e2020GL087291. https://doi.org/10.1029/2020GL087291

Vijay, S., King, M. D., Howat, I. M., Solgaard, A. M., Khan, S. A., & Noël, B. (2021). Greenland ice-sheet wide glacier classification based on two distinct seasonal ice velocity behaviors. *Journal of Glaciology*, *67*(266), 1241–1248. https://doi.org/10.1017/jog.2021.89

Werder, M. A., Hewitt, I. J., Schoof, C. G., & Flowers, G. E. (2013). Modeling channelized and distributed subglacial drainage in two dimensions. *Journal of Geophysical Research: Earth Surface*, *118*(4), 2140–2158. https://doi.org/10.1002/jgrf.20146

Wood, M., Rignot, E., Bjørk, A., van en Broeke, M., Fenty, I., Menemenlis, D., et al. (2020). Greenland marine-terminating glacier retreat data. [Dataset]. *Dryad*. https://doi.org/10.7280/D1667W

Wood, M., Rignot, E., Fenty, I., An, L., Bjørk, A., van den Broeke, M., et al. (2021). Ocean forcing drives glacier retreat in Greenland. *Science Advances*, *7*(1), eaba7282. https://doi.org/10.1126/sciadv.aba7282